Available online www.jocpr.com

Journal of Chemical and Pharmaceutical Research, 2013, 5(6):50-59

Research Article

ISSN : 0975-7384
CODEN(USA) : JCPRC5

Synthesis and characterization of 2-amino pyridine dithiocarbamate ligand and it's Cu(II), Co(II) metal complexes

K. Venu Gopal*, P. Siva Jyothi, P. Ashok Gajapathi Raju, K. Rameshbabu and J. Sreeramulu

Dept. of Chemistry, Sri Krishnadevaraya University, Anantapur, A.P., India

---

ABSTRACT

New series of bidentate ligand dithocarbamate of 2–Amino pyridine (2APDTC) have been synthesized by new synthetic methods as it's sodium salt. In the reaction of Copper Chloride and Cobalt Chloride with 2APDTC the corresponding complexes were prepared. The complexes were characterized by elemental analysis, IR, ^{1}H NMR, UV, ESR, Powder X-ray diffraction and TGA – DTA. These metal complexes show moderate and selective activity towards some of the test microorganisms.

Keywords: 2–Amino pyridine, Copper Chloride, Cobalt Chloride, Dithiocarbamates, Synthesis, Characterization, Anti bacterial activity.

INTRODUCTION

Dithiocarbamates deals with a great interest in organic synthesis as they are important synthetic intermediates and they can be found in a variety of biologically active compounds . For example, they can act as fungicides to protect crops from fungal diseases. These compounds have a number of other applications in photochemistry, as catalyst in the sulfur vulcanization of rubber, and numerous biological and medicinal properties including applications in the treatment of cancer, play pivotal roles in agriculture and act as linkers in solid-phase organic synthesis. [1-16].Metal complexes of dithiocarbamates with nitrogenous bases such as 1,10-phenanthroline, 2,2'-bipyridine and its derivatives have been reported[17-25] In view of the wide range of applications of dithiocarbamates [26]. we report in this article the synthesis and characterization of 2-Amino pyridine dithiocarbamate ligand and its Cu (II) and Co (II) metal complexes. Antimicrobial activities of the complexes were investigated *in vitro*.

EXPERIMENTAL SECTION

All materials used in this investigation were purchased from Sigma/Aldrich and AR (Merck). Solvents used were of reagent grade and purified before use by the standard methods Cu[2APDTC], Co[2APDTC] complexes were prepared by the procedures described in the literature. Conductivity measurements of the above Cu and Co complexes were carried out on a systronics conductivity bridge 303, using a conductivity cell of cell constant 1.0. The dithiocarbamate metal complexes of Copper (II) and Cobalt (II) were soluble in dimethyl formamide (DMF). Infrared spectra of the metal complexes were recorded on a Perlan – Elmer IR 598 spectrometer (4000 – 200 cm^{-1}) using KBr Pellets. The ESR spectrum of copper complex was recorded, by using JEOL, JES FA 200 EST spectrometer, at HCU, Hyderabad. Microchemical analysis of Carbon, Hydrogen and Nitrogen for the complexes were carried out as a Herause CHNO–RAPID elemental analyzer. ^{1}HNMR spectra were recorded on av – 400 MHZ NMR spectrometer in IISC, Bangalore in DMSO–d6 solvent. Melting points were determined on a unimelt capillary melting point apparatus.

Preparation of Sodium salt of dithiocarbamate ligands:
0.05mol of amine was dissolved in 10ml of absolute alcohol in a clean beaker which was placed in ice. To this cold solution 5ml of sodium hydroxide (10N) solution was added and then pure carbondisulphide (3.02ml, 0.05mol) was added in drop wise through separating funnel with constant stirring. The components were stirred mechanically for about 30min, sodium salt of dithiocarbamate precipitated out. It was dried and recrystallised from methanol.

Synthesis of Dithiocarbamate Metal Complexes
The aqueous solution of 0.005mol of metal salts was added with constant stirring to an aqueous solution of 0.01 sodium dithiocarbamate ligand. The reaction mixture was stirred at room temperature for 8 hours. The colored precipitate was obtained. The precipitate was filtered and washed with water and then with methanol and dried over calcium chloride in a desiccator. All the complexes were prepared in 1:2 ratios of metal to ligand.

The elemental analysis data of [2APDTC] is as follows. Yield 79% and decomposes at 115^{o}C Anal. Calcd. For C–45.90%, H –3.83%, N–15.30%, S - 34.97% Found C–45.13%, H–3.49%, N–14.86% S -34.12%

The elemental analysis data of Cu[2APDTC] is as follows. Yield 65% and decomposes at 227^{o}C Anal. Calcd. For C–36.09%, H –3.87%, N–12.03%, S - 27.49% Found C–35.26%, H–3.63%, N–11.37% S -26.56%

The elemental analysis data of Co[2APDTC] is as follows. Yield 58% and decomposes at 220^{o}C Anal. Calcd. For C–36.45%, H –3.90%, N–12.15%.A – 27.77% Found C–35.78%, H–3.43%, N–11.29%. S- 27.03%.

RESULTS AND DISCUSSION

3.1. I.R. Analysis of the Ligand

The typical I.R spectrum of 2APDTC ligand is presented in the Fig. 1(a). The most significant bands recorded in the FT–IR spectra of the ligand and its metal complexes are reported in the Table 1.

As concern the 2–aminopyridine dithiocarbamate moiety, two main regions of the IR were considered.

First, the (1451–1550 cm^{-1}) region, which is primarily associated with υ (N–CSS) stretching vibrations. Second, the 950–1000 cm^{-1} region, which was associated with υ(C–S) stretching vibrations.

The characteristic band at 1481.03 cm^{-1}, was assignable to υ(N–CSS) this band defines a carbon Nitrogen bond order between a single bond (υ =1250–1350cm^{-1}) and a double bond (υ =1640–1690cm^{-1}). The appearance of a band in that region indicates that, of the three possible resonance structures reported by Chart et al., characterized by a strong delocalization of electrons in the dithiocarbamate moiety. A sharp band at 995.48 cm^{-1} associated with the υ(N–H) stretching vibrations and the band at 1596.68 cm^{-1} was associated with the υ(N=C) bond stretching in the pyridine ring.

I.R. Characterization of Metal Complexes

The interpretation of IR spectra of dithiocarbamates complexes of Transition metals had arisen considerable interest both diagnostically to determine the mode of co–ordination and as a mean of assessing the nature of bonding in these complexes. The Infrared spectrum of Cu (II) & Co (II) complexes was compared with the [2APDTC] ligand. The typical I.R spectra of [2APDTC] complexes were presented in Fig 1(b) and 1 (c).

For dithiocarbamate complexes three main regions of IR are of interest. First, the 1580–1450 cm^{-1} region. This was primarily associated with the stretching vibrations of C–N group of N–CSS– moiety. A strong band exhibited at 1481.03 cm^{-1} in the I.R spectrum of the ligand, which was assigned to the thioureide bond is shifted higher regions 1532.89 and 1519.64 cm^{-1} for Cu(II) and Co(II) complexes respectively, suggesting the complexation of ligand with metal ion. On Passage from the free dithiocarbamate ligand to their complex, the υ(N–CSS) mode is shifted to higher energies, showing an increase of Carbon–Nitrogen double bond character.

The Infrared active υ(N–CSS) mode was sensitive to both chain length and the steric bulk of the substituents. As double character was more pronounced in the complex it can be concluded that the ligand was coordinated through both the sulphur atoms.

The Second region of consideration was 950–1050 cm^{-1}, to discern the bonding type of the dithiocarbamate ligand in their complexes, the Bonati–Ugo method is, by far, the most popular one. It consists of tracing the 940–1060 cm^{-1} spectral region, where the υ(C–S) modes were thought to appear. In fact, the bands due to –CSS moiety is usually coupled to other vibrations and is very sensitive to the environment around this group, but they were also useful to distinguish between Monodentate and Bidentate Coordination. The presence of only one band in the investigated region, commonly attributed to υ(SCS) mode, it indicates completely symmetrical bonding of the dithiocarbamate ligand to Metal in bidentate mode where as a doublet is expected for the Monodendate coordination.

Basing on the above concept the presence of single band at 1027.30 cm^{-1} and 1033.30 cm^{-1} region was assumed to υ(C–S) stretching vibrational mode and it indicates the symmetric bidentate behavior of the ligand.

Along with these bands new bands were formed in spectra of complexes in the region 394.58 cm^{-1} and 379.12 cm^{-1}, were assigned to υ(M–S) modes for Cu & Co respectively.

The appearance of a broad band in the region 3343.58–3412.58 cm^{-1} can be assigned to the υ(O–H) stretching vibrations of coordinated water molecules present in the complex.

Table: (1) The important IR Bands of the Ligand and its metal complexes

Name of the compound	Thioureide bond	–OH (water)	C–S	M–S
L=2A3MPDTC	1481.03	–	998.44	–
$[Cu(L)_2(H_2O)_2]$	1532.89	3343.58	1027.27	394.58
$[Co(L)_2(H_2O)_2]$	1519.64	3412.58	1033.89	379.12

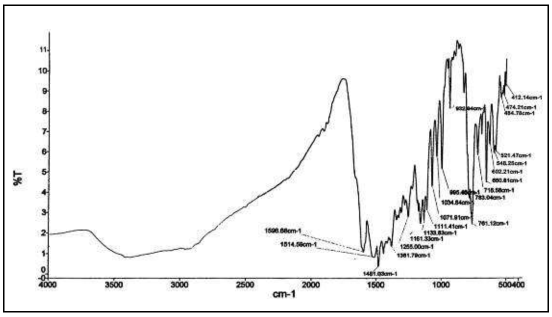

Fig. 1(a) : IR spectrum of the 2APDTC ligand

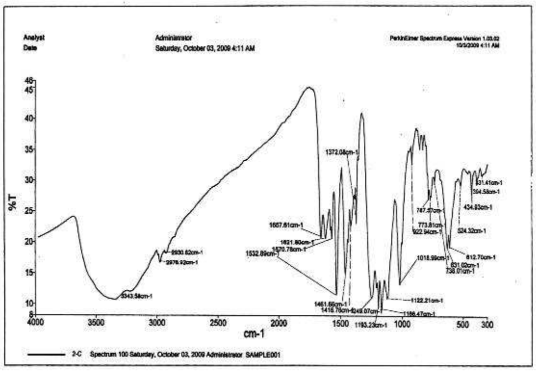

Fig. 1(b) : IR spectrum of the Cu[2APDTC] metal complex

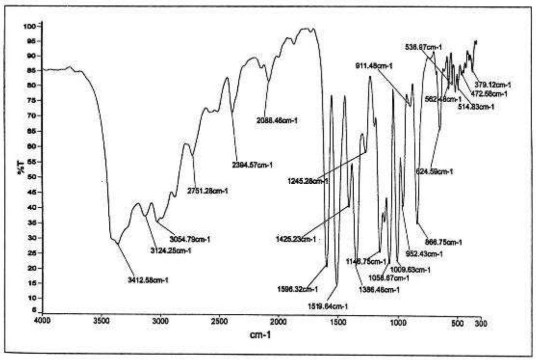

Fig. 1(c) : IR spectrum of the Co[2APDTC] metal complex

3.2. ^{1}H–NMR Spectral Studies

Fig.2(a) Depict the noted important chemical shift values of the ligand, these values were summarized in Table 2.

Fig. 2(a) gives the typical NMR spectrum of the ligand 2APDTC. The peaks in the aromatic region were seen as a set of multiplets in the range 7.2-7.6 ppm and the signal due to proton attached to the nitrogen, in thioureide bond was appeared as a broad singlet at 10.5 ppm.

Fig. 2(b) and Fig. 2(c), gives the typical NMR spectrum of the [2APDTC] Cu and [2APDTC] Co respectively. In the complexes, signal due to proton bonded to Nitrogen in thioureide bond was observed in the range 10.94-10.81 ppm. The down field shift of the complex may attributed to an increase of the II - bond character and the delocalization of electron along the C-N bond contributed by the substituents and also the bidentate nature of the dithiocarbamate ligand. On complexation, the electron density on -NH decreases, the processional frequency of proton bonded to Nitrogen increases, hence the signal was shifted to down field regions.

It was observed that the aromatic ring protons of range 7.2-7.6 ppm become broad and less intensive when compared to the corresponding dithiocarbamatee ligand. This effect may be due to the drifting of ring electrons towards the metal ion.

The broad signal in the range ppm 8.95-9.5 ppm in the case of metal complex indicates the complexation of water molecule to metal ion.

Table (2). ^{1}H–NMR spectral data of ligand & its metal complexes in DMSO-d$_6$ in ppm

Name of the compound	H-N-C Thioureide bond	OH Coordinated water	Py-H
L=2A3MPDTC	10.4	-	7.2-7.6
$[Cu(L)_2(H_2O)_2]$	10.94	9.5	7.5-8.0
$[Co(L)_2(H_2O)_2]$	10.81	9.8	7.3-7.8

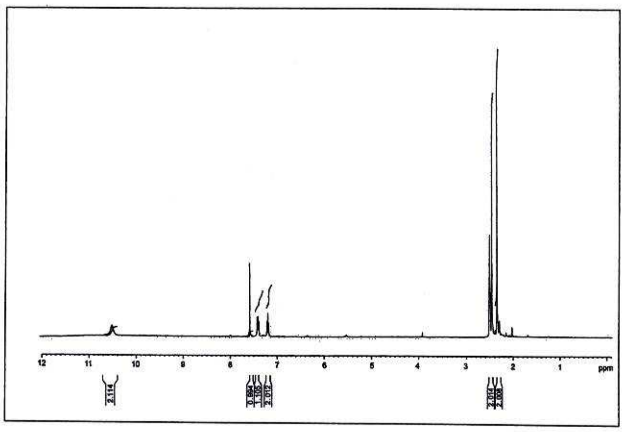

Fig.2(a). ^{1}H NMR spectrum of the 2APDTC ligand in DMSO-d$_6$ solvent

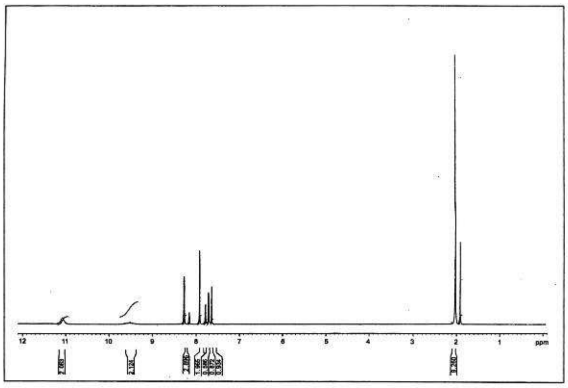

Fig.2(b). ^{1}H NMR spectrum of the Cu2APDTC ligand in DMSO-d$_6$

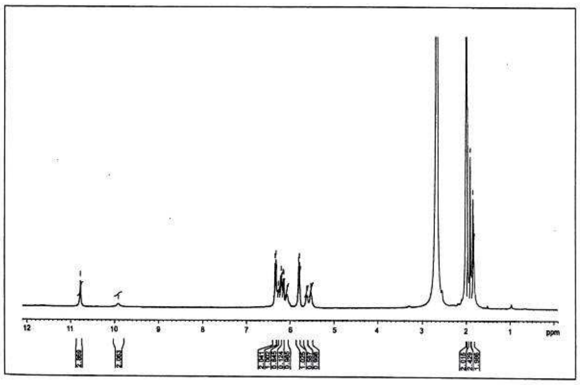

Fig.2(c). ^{1}H NMR spectrum of the Co2APDTC ligand in DMSO-d$_6$

3.3. UV – Visible Spectral Studies

The solution electronic spectra of the ligand and the complexes were recorded in DMF as solvent in the UV-Visible region. The electronic transition data was given in the Table 3.

Fig. 3(a) shows the electronic spectra of the sodium 2-amino pyridine dithiocarbamate, it shows two strong absorption bands at 239 nm and 276 nm. These bands may be due to n→π* and π →π* transitions of $N \cdots C \cdots S$ group and n→π* electronic transition involving lone parr of electrons located on the sulphur atom. On complexation these bands were shifted to lower wavelength. In the complexes, bands below 300 nm are attributed to the intraligand transitions.

The Electronic spectrum of the Cu-2APDTC complex was shown in the Fig. 3(b). It exhibits an intense band at 265 nm with a shoulder at 326 nm were assigned to the intramolecular charge transfer of the ligand ($\pi \rightarrow \pi^*$ and $n \rightarrow \pi^*$ in the N-C=S group). A moderately intense peak observed at 397 nm may be due to the charge transfer [LMCT]. The weakest band in the higher wavelength region can be attributed to d→d metal orbital transitions. In particular this broad band can be assigned to the $d_{x^2-y^2} \rightarrow d_{xy}$ and $d_{x^2-y^2} \rightarrow d_{xz,\ yz}$ transitions. In an octahedral crystal field, the corresponding ground state electronic configuration is $t_{2g}^6 e_g^3$ which yields ^2E_g term. The excited electronic configuration, $t_{2g}^5 e_g^4$ corresponds to $^2T_{2g}$ term. Thus only one single electronic transition $^2E_g \rightarrow {}^2T_{2g}$ was expected in an octahedral crystal field. Based on the spectral data it was shown that the copper complex forms octahedral complex.

The Electronic spectrum of the Co-2APDTC complex was shown in the Fig. 3(c). It shows two intense bands and one less intense shoulder band. The intense bands at 271 nm with a shoulder at 285 nm and another moderate intense band at 345 run were ascribed to the to the intramolecular charge transfer of the ligand ($\pi \rightarrow \pi^*$ and $n \rightarrow \pi^*$ in the N–C=S group). A moderately intense peak observed at 381 nm may be due to the ligand-metal charge transfer [LMCT. The Cobalt complex shows two less intense broad bands in the high wave length region corresponding to intraligand d→d metal orbitals transitions. In particular this broad band can be assigned to the $d_{xy} \rightarrow d_{x^2-y^2}$ and $d_{xz,\ yz} \rightarrow d_{x^2-y^2}$ transitions.

Table (3) UV-Vis spectral data of the ligands and its metal complexes

Compound	λ_{max}	Possible assignment
L= 2APDTC	239 nm and 276 nm	$\pi \rightarrow \pi^*$, $n \rightarrow \pi^*$
$[Cu(L)_2(H_2O)_2]$	265, 326	$\pi \rightarrow \pi^*$
	397	LMCT
	535	d–d
$[Co(L)_2(H_2O)_2]$	271, 285	$\pi \rightarrow \pi^*$
	345	LMCT
	381	d–d

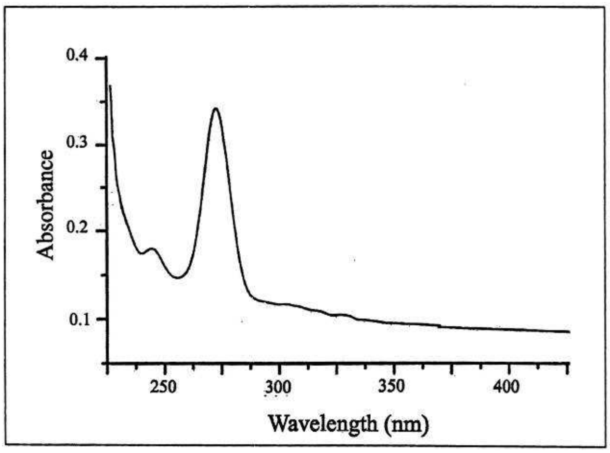

Fig. 3(a). UV- Vis spectrum of the 2APDTC ligand

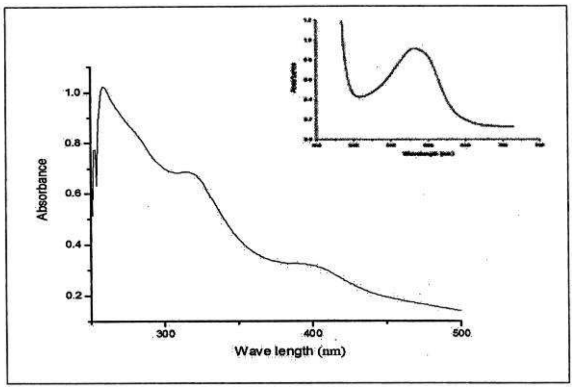

Fig. 3(b). UV- Vis spectrum of the Cu[2APDTC] metal complex

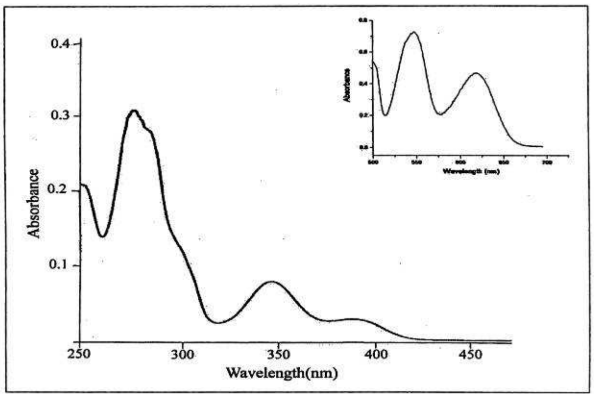

Fig. 3(c). UV- Vis spectrum of the Co[2APDTC] metal complex

3.4 .ESR Spectral analysis of [2AMPDTC] Cu complex

ESR spectra obtained for copper complex in DMF at liquid nitrogen temperature and representative ESR spectrum was presented in Fig.4. In this low temperature spectrum, three peaks of small intensity have been identified which are considered to originate from $g\|$ component. The spin Hamiltonian, orbital reduction and bonding parameters of the complex were given in Table.4.

Kivelson & Neiman have reported that $g\|$ value is less than 2.3 for covalent character and it is greater than 2.3 for ionic character of the metal-ligand bond in complex, Applying this criterion, the covalent bond character can be predicted to exist between the metal and the ligand for complex.

The g tensor value of the copper complex can be used to derive the ground state. The trend $g\| > g_{ave} > g\perp > 2.0023$ observed for the complex suggests that the unpaired electron was localized in $d_{x^2-y^2}$ orbital of the copper (II) complex. The lowest g value (>2.0027) also consistent with $d_{x^2-y^2}$ ground state. The $g\|/A\|$ quotient value was 102.41 cm, evidence in support of the octahedral geometry with no appreciable distortion.

The Axial symmetry parameter G value was calculated by using the expression, $G = g\|-2/ g\perp-2$ and related to the exchange interactions between copper -copper centers, according to Hathway, for the present complex the G=4.54, indicates the formation of monomeric complexes. The ESR parameters $g\|$, $g\perp$, $A\|^*$, and $A\perp^*$ of the complex and the energies of d-d transitions were used to evaluate the orbital reduction parameters ($K\|$, $K\perp$). According to Hathway the observed $K\| < K\perp$ indicates the presence of significant in plane Π-bonding. The molecular orbital coefficients or the bonding parameters α^2 (in plane σ-bonding) and β^2 (in plane π-bonding) were calculated. The observed α^2 value for the present chelate 0.5780 indicates that the complex was having some covalent character.

The reduction of P value from the free ion value (0.036 cm^{-1}) might be attributed to the strong covalent bonding. The Fermi constant interaction term (K) indicates the interaction between the electronic and the nuclear spins give n by the expression $K=A_0/(P-\Delta g_0)$, where ($\Delta g_0= g_e-g_0$), it represents the amount of unpaired electron density at the nucleus. The lower P and α^2 values for Cu [2APDTC] complex suggest the presence of strong in-plane Π bonding which in agreement with higher ligand field. The shape of ESR lines, ESR data together with the electronic spectral data suggest octahedral geometry for copper complex.

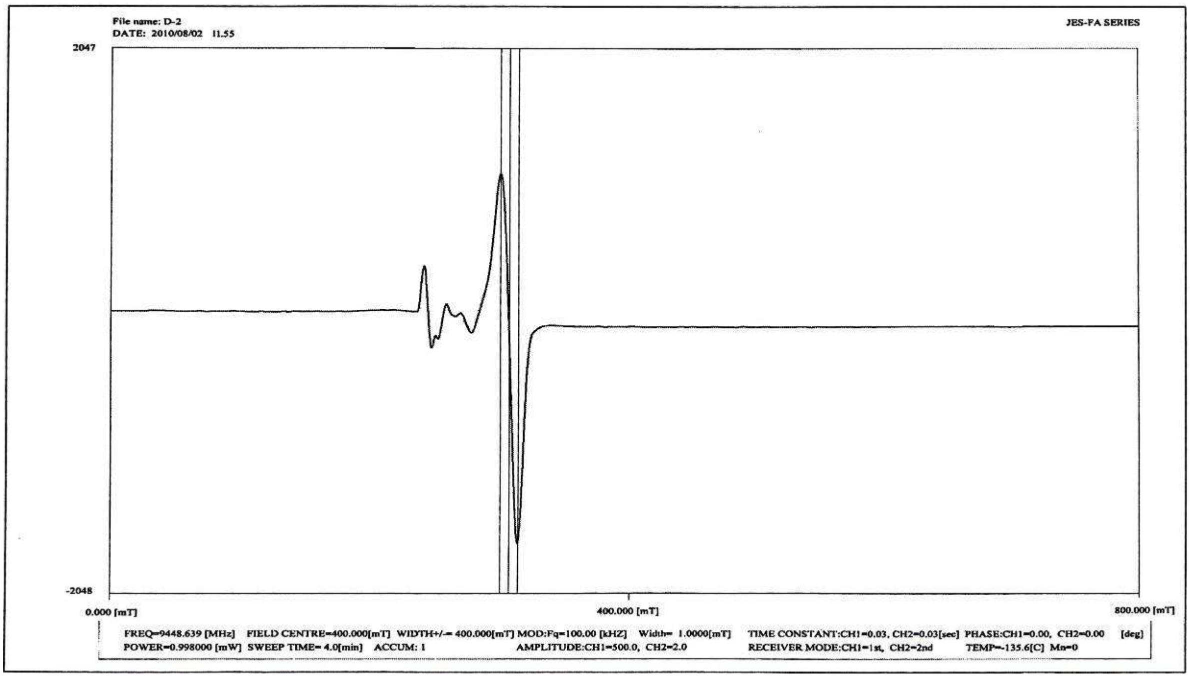

Fig. 4. ESR spectrum of the Cu[2APDTC] metal complex

3.5. Thermal Studies of metal complexes

[2APDTC] Cu & [2APDTC] Co complexes

TG techniques were employed to follow the thermal behavior of complexes. According to the results obtained, the complexes are not volatile and their decomposition occurs in more than one step. The typical thermogram of complexes is shown in the Fig, 5(a). and 5(b). Thermogravimetric studies on the complexes confirmed their proposed molecular formulae. The thermal decomposition of metal complexes has been followed up to 1000°. The decomposition behavior of the complexes is observed in nitrogen atmosphere. The experimental mass losses were in good agreement with the calculated mass loss values which are summarized in the Table.5.

Table. (4) Spin Hamiltonian and orbital reduction parameters of Copper complex in DMF solution

Parameters	Cu $(2APDTC)_2$
$g_\parallel$	2.294
$g_\perp$	2.0613
g_{ave}	2.1388
G	4.796
$A_\parallel^*$	0.0224
$A_\perp^*$	0.00171
A^*_{ave}	0.0086
d–d	18691
$K_\parallel$	0.7135
$K_\perp$	0.8343
P*	0.02414
α^2	0.5583

* *values are given as* cm^{-1} *units.*

The Copper complex shows three main decomposition stages, and the first stage with small endothermic dehydration step in the range of 98.23°C to 123.56°C is due to loss of two water molecules coordinated to the metal. The Second step involves two sub steps which involves decomposition of the ligand moiety, Exothermic decomposition of the ligand moiety takes place around 224.67-297.243°C, to give the stable intermediate M $(SCN)_2$ and this was stable up to 535.26°C, which on further undergoes exothermic decomposition in the region 535.26-578.83 °C in the third stage forming Copper sulphides (CuS) as final residual product.

The thermogram of the Cobalt complex shows First stage of decomposition around 96.42°C to 115.56°C, which indicates the presence of coordinated water molecules and this decomposition corresponds to small endothermic dehydration of the complex and gives anhydrous complex. The second decomposition stage with one broad exothermic peak corresponds to the degradation of ligand moiety in the region 245.78°C to 395.34°C forming $M(SCN)_2$ intermediate. This on subsequent stages undergoes exothermic decomposition to give the corresponding cobalt sulphide as the final decomposition product at a high temperature above 779.54°C.

Table. (5) Thermo analytical data of metal complexes

Complex X=H_2O	Temperature range in °C	Probable assignment	Mass loss (%)	Total mass loss (%)
Cu L_2 2X L=$C_6H_5N_2S_2$	98.23-123.56 224.67-297.24 535.26-578.83	Loss of $2H_2O$ molecules Decomposition of L Formation of CuS	8.13 50.74 19.05	77.92
Co L_2 2X L=$C_6H_5N_2S_2$	96.42-115.56 245.78-395.34 523.15-779.54	Loss of $2H_2O$ molecules Decomposition of L Formation of CoS	8.254 51.285 19.40	78.939

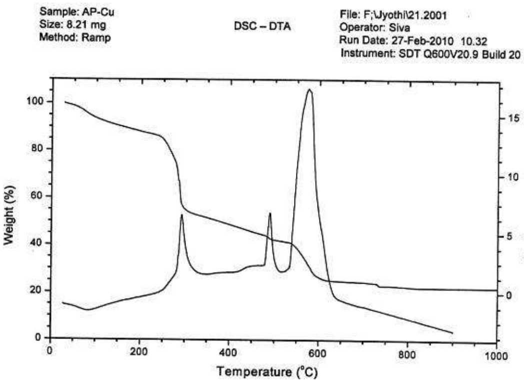

Fig. 5(a). Thermogram of the Cu[2APDTC] metal complex

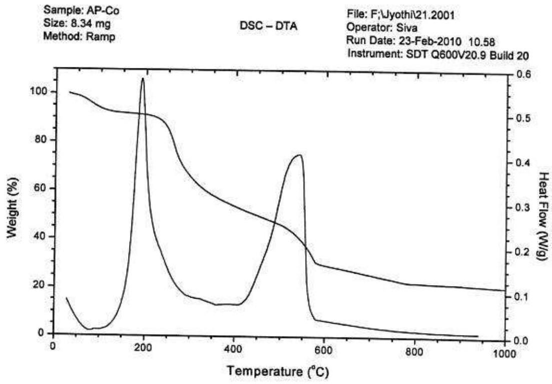

Fig. 5(b). Thermogram of the Co[2APDTC] metal complex

3.6. Powder X ray diffraction Studies of 2APDTC metal complexes

For Copper complex the diffractogram record 23 diffractions and for Cobalt complex the diffractogram record 15 diffractions, the representative X RD spectra of Cu and Co metal complex were shown in Fig. 6(a) and Fig. 6(b) respectively. 2θ values were ranging 2-60, where θ-is the Bragg's angle. All the main peaks were indicated and calculated values of Miller indices (h k 1) along with observed d-spacing and 2θ were specified in the Table. 6(a), 6(b). All the peaks had been indexed and 2θ values compared in graph. Comparison values revels that there was good agreement between values of 2θ and d-values. The powder X-ray diffraction data showed identical features with very poor crystallinity. The patterns were qualitative and dispersive in intensity for Copper and Cobalt metal complexes. The diffraction patterns of the complex had been indexed by standard methods and the (h k 1) values were calculated from the indexed data by trial and error method.

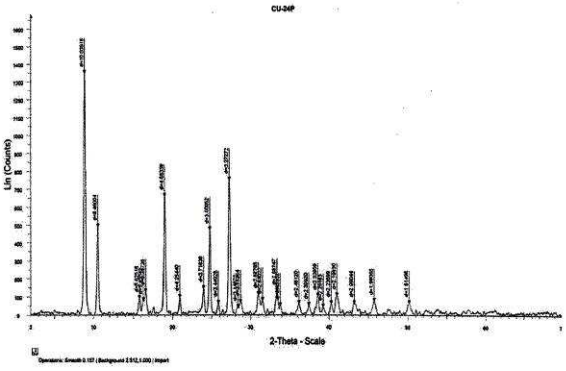

Fig. 6(a). X–ray diffractogram of the Cu[2APDTC] metal complex

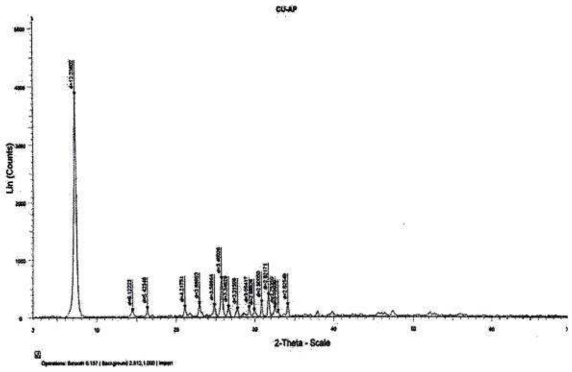

Fig. 6(b). X–ray diffractogram of the Co[2APDTC] metal complex

Table. 6(a). Powder X Ray diffraction data of the complex Cu [2APDTC]

lane	d expt	calc	2θ expt	calc	h	k	1
1	7.45291	7.4362	12.1664	12.034	2	2	0
2	6.8953	6.86741	13.9063	13.885	3	1	1
3	5.9438	5.8795	14.892	14.231	3	2	2
4	5.64442	5.65126	15.687	15.673	3	3	0
5	5.5944	5.4789	15.828	15.893	4	2	0
6	5.32091	5.31902	16.648	16.546	4	2	2
7	5.2487	5.0134	16.879	16.729	5	0	0
8	4.9863	4.8124	17.774	17.723	5	2	1
9	4.6388	4.5893	19.117	19.015	5	2	2
10	3.7331	3.6245	23.816	23.709	5	4	2
11	3.6507	3.5231	24.362	24.119	6	2	0
12	3.4382	3.3218	25.893	25.215	6	2	2
13	3.1637	3.0241	28.184	28.102	6	4	0
14	3.0251	3.0073	29.504	29.219	7	3	1
15	2.94861	2.85673	30.287	30.216	7	3	3
16	2.88437	2.78345	30.979	30.783	8	2	0
17	2.83835	2.82417	31.494	31.482	8	2	2
18	2.3894	2.37924	37.614	37.562	7	5	1
19	2.37466	2.31973	37.856	37.105	7	5	3
20	1.77498	1.68524	51.44	51.321	8	4	0
21	1.77311	1.76903	51.499	51.481	8	4	2
22	1.61234	1.60946	54.789	54.771	7	5	5
23	1.60598	1.60042	58.932	58.832	9	1	1

Table. 6(b). Powder X Ray diffraction data of the complex Co [2APDTC]

lane	d expt	calc	2θ expt	calc	h	k	1
1	10.28013	10.2621	8.595	8.435	2	0	0
2	8.95941	8.9245	9.864	9.742	1	1	1
3	4.55364	4.5423	19.478	19.266	2	2	0
4	4.52524	4.5234	19.602	19.291	3	1	1
5	4.48468	4.4765	19.781	19.327	4	2	0
6	3.15658	3.1232	28.249	28.081	3	3	1
7	3.1227	3.1007	28.562	28.429	3	3	3
8	3.10381	3.0652	28.74	28.725	4	2	2
9	3.08653	3.0711	28.904	28.531	5	1	1
10	3.06468	3.0843	29.115	28.942	5	3	1
11	3.04679	3.0216	29.289	29.034	6	2	0
12	2.96824	2.9145	30.082	29.995	6	4	2
13	1.81205	1.8064	50.314	50.021	7	3	1
14	1.77611	1.7629	51.405	51.115	7	3	3

4. Antibacterial activity

The present investigation was an attempt to find out antibacterial activity of ligand and their metal complexes against *Escherichia coli*, *Staphylococcus aureus* and *Bacillus subtilis* in the range 50–150 um/ml. Choosing serial paper disc diffusion method. The antibacterial activity results were given in the table 7. The high antimicrobial activities of all the newly synthesized metal complexes surmounting that of ligands showed that complexation of the organic moiety to the metal ions substantially enhanced their activities. Such increased activity of metal chelates had been explained by Overtones concept and the Tweedy's chelation theory. On chelation the polarity of the metal ion reduced to a greater extent due to the overlap of the ligand orbital and partial sharing of positive charge of metal ion with donor groups. It was further noted that the delocatlization of Π–electrons over the whole chelate ring enhanced the lipophillicity of the complexes. This increased lipophillicity enhanced the penetration of the complexes into lipid membrane and blocking the metal binding sites on enzymes of microorganism thus retarding the normal cell processes.

Table 7 : Antibacterial activities of ligand and their transition metal complexes (Zone formation in mm)

Compound	*Escherichia coli*	*Staphylococcus aureus*	*Bacillus subtilis*
2APDTC	6	7	8
$(2APDTC)_2Cu$	9	11	12
$(2APDTC)_2Co$	8	10	9

CONCLUSION

By concluding the above information the different dithiocarbamate ligand of 2–amino pyridine, acts as good complexing agents towards many transition metal ions. By using all the above mentioned analytical data it was concluded that they behave as symmetric bidendate ligand during complexation. All the metal complexes carry no charge and are thermally stable. As such no single technique is independent of predicting final structures of the complexes, the entire information available from all the studies were clubbed together and suggested structures of the complexes for mentioned as follows:

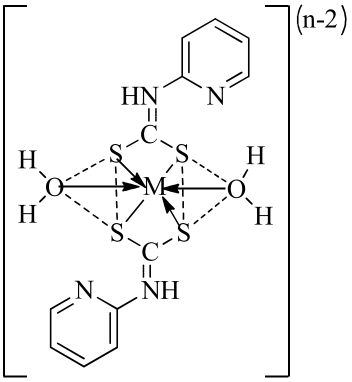

M[2APDTC]; M = Cu(II) & Co(II)

REFERENCES

[1] M. Dhooghe, N. D. Kimpe., *Tetrahedron.*, **2006**, **62**, 513.
[2] A. W. Erian, S. M. Sherif., *Tetrahedron.*, **1999**, **55**, 7957.
[3] R. D. Norcross, I. Paterson., *Chem. Rev.*, **1995**, **95**, 2041.
[4] D. J. Faulkner., *Nat. Prod. Rep.*, **1995**, **12**, 223.
[5] G. Liu, J. T. Link, Z. Pei, E. B. Reilly, S. Leitza, B. Nguyen, K. C. Marsh, G. F. Okasinski, T. W. V. Geldern, M. Ormes, K. Fowler, M. Gallatin., *J. Med. Chem.*, **2000**, **43**, 4025.
[6] R. S. Grainger, P. Innocenti; *Heteroat. Chem.*, **2007**, **18**, 568.
[7] W. D. Rudorf; *J. SulfurChem.*, **2007**, **28**, 295.
[8] A. R. Katritzky, S. Singh, P. P. Mohapatra, N. Clemens, K. Kirichenko., *Arkivok.*, **2005**, **ix**, 63.
[9] T. Kondo, T. A. Mitsudo., *Chem. Rev.*, **2000**, **100**, 3205.
[10] W. Schwack, R. C. Perz, H. Lishaut; *J. Agric. Food Chem.*, **2000**, **48**, 792.
[11] C. Len, P. Villa, G. Ronco; *J. Agric. Food Chem.*; **2000**, **48**, 5283.
[12] E. D. Caldas, M. H. Conceicao, M. C. Miranda, L. Souza, J. F. Lima., *J. Agric. Food Chem.*, **2001**, **49**, 4521.
[13] V. F. Plyusnin, V. P. Grivin and S. V. Larionov., *Coord. Chem. Rev.*, **1997**, **159**, 121.
[14] M. R. Saidi, N. Azizi, F. Ebrahimi, E. Aakbari and F. Aryanasab., *Synlett.*, **2007**,2797.

[15] N. Azizi, F. Aryanasab, L. Torkiyan, A. Ziyaei-Halimjani, M. R. Saidi., *J. Org. Chem.*, **2006**, **71**, 3634.
[16] S. Xia, X. Wang, Z. Ge, T. Cheng and R. Li., *Tetrahedron*; **2009**, **65**, 1005.
[17] JL Serrano; L García; J Pérez; E Pérez; G Sánchez; J García; G López; G García; E Molins. *Inorg. Chim. Acta*, **2003**, 355, 33140.
[18] L Giovagnini; C Marzano; F Bettio; D Fregona. *J. Inorg. Biochem.*, **2005**, 99, 2139–2150.
[19] KS Siddiqi; SAA Nami; Lutfullah; Y Chebude. *Synth. React. Inorg. Met.-Org. Nano-Met.Chem.*, **2005**, 35, *6*, 445-451.
[20] A Manohar; K Ramalingam; R Thiruneelakandan; G Bocelli; L Righi. *Z. Anorg. Allgem.Chem.*, **2006**, 632, 461-464.
[21] BA Prakasam; K Ramalingam; G Bocelli; A Cantoni. *Bull. Chem. Soc. Japan*, **2006**, 79, *1*,113-117.
[22] BA Prakasam; K Ramalingam; R Baskaran; G Bocelli; A Cantoni. *Polyhedron*, **2007** 1133-1138.
[23] R Pastorek; J Kameníček; J Husárek; V Slovák; M Pavlíček. *J. Coord. Chem.*, **2007**, 60, *5*,485-494.
[24] Z Trávníček; R Pastorek; V Slovak. *Polyhedron*, **2008**, 27, 411-419.
[25] R Baskaran; K Ramalingam; G Bocelli; A Cantoni; C Rizzoli. *J. Coord. Chem.*, **2008**, 61, *11*, 1710–1719.
[26] MR Chaurasia; AK Sharma; SK Sharma. *J. Indian Chem. Soc.*, **1981**, LVIII, 687–689